Surface nanostructures by single highly charged ions

2009 J. Phys.: Condens. Matter 21 224012

(http://iopscience.iop.org/0953-8984/21/22/224012)

J. Phys.: Condens. Matter **21** (2009) 224012 (9pp) doi:10.1088/0953-8984/21/22/224012

Surface nanostructures by single highly charged ions

S Facsko[1], R Heller[1], A S El-Said[2], W Meissl[3] and F Aumayr[3]

[1] Institut für Ionenstrahlphysik und Materialforschung, Forschungszentrum Dresden-Rossendorf, D-01328 Dresden, Germany
[2] Physics Department, Faculty of Science, Mansoura University, 35516 Mansoura, Egypt
[3] Institut für Allgemeine Physik, TU Wien, A-1040 Vienna, Austria

E-mail: S.Facsko@fzd.de

Received 8 January 2009, in final form 11 February 2009
Published 12 May 2009
Online at stacks.iop.org/JPhysCM/21/224012

Abstract

It has recently been demonstrated that the impact of individual, slow but highly charged ions on various surfaces can induce surface modifications with nanometer dimensions. Generally, the size of these surface modifications (blisters, hillocks, craters or pits) increases dramatically with the potential energy of the highly charged ion, while the kinetic energy of the projectile ions seems to be of little importance. This paper presents the currently available experimental evidence and theoretical models and discusses the circumstances and conditions under which nanosized features on different surfaces due to the impact of slow highly charged ions can be produced.

(Some figures in this article are in colour only in the electronic version)

1. Introduction

Ion beams are used extensively in etching (erosion), implantation or modification of solid surfaces. Semiconductor technology as well as other technologies are not imaginable without these techniques [1]. Recently, it has been demonstrated that regular patterns with lateral periodicity less than 50 nm can be produced by ion beam erosion in a self-organized mask-less manner, opening new opportunities for nanotechnology ([2] and articles in this special topic volume). In the case of singly charged ions at low to moderate kinetic energy ($E_{kin} < 5$ keV) the interaction with the solid is dominated by collisions between the projectile and the target nuclei and the energy is mainly dissipated by nuclear energy loss. The main interaction mechanisms in this regime are nuclear collisions leading to defect creation, intermixing and surface sputtering [3].

With increasing charge state the ions carry more and more *potential energy*, i.e. the sum of the ionization energies to charge the ion, and effects dominated by the release of this energy become important [4]. In figure 1 the potential energy of Ar and Xe as a function of their charge state is shown as an example. For high charge states the amount of potential energy deposited into the surface can greatly exceed the deposited kinetic energy and can reach values beyond 100 keV. The potential energy is released differently from the kinetic energy of the ion, i.e. in electronic exchange interactions. Thereby an excitation of the electronic system of the solid is induced. Consequently, many effects related to the potential energy of HCI have been observed in the past, e.g. potential electron emission [5–7] and potential sputtering [8].

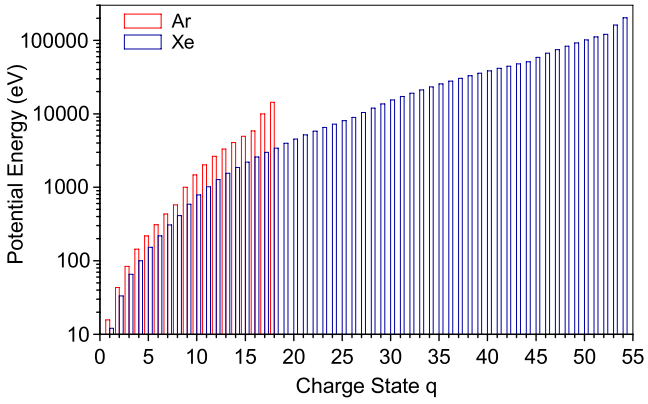

Figure 1. Potential energy (sum of the ionization energies) of Ar^{q+} and Xe^{q+} ions as a function of the charge state q.

The interesting aspect of the potential energy release is the high electronic excitation comparable to the excitation with

high power laser pulses or particles with much higher kinetic energy (swift heavy ions) with the essential difference that, in the case of an HCI, the excitation is strongly localized at the surface in a volume of only a few nm^3. Therefore, local phase transformations may occur which can be identified as permanent surface modifications [9]. From the point of view of applications the advantages of HCI for surface modifications are the high local excitation not accessible with conventional beams and the high surface selectivity when using ions with low kinetic energy. This combination makes HCI promising for surface analysis [10] and as a gentle tool for surface modification [11]. At present the structures produced by HCI are randomly distributed over the surface and the studies done so far are dealing mainly with the fundamental understanding of the mechanisms involved. For establishing HCI as a future tool for nanostructuring it would be highly desirable to control the shape and the position of the structures, which will be the next step in the development of this technique [12].

This paper focuses on surface modifications induced by the potential energy of HCI, contrasting the modifications accompanying the nuclear collision cascade or excitation by the electronic energy loss of the ions.

2. Relaxation of HCI at surfaces

The surface modifications induced by the released potential energy of HCI results from an electronic excitation in the surface. In the following a brief review of the current understanding of the interaction of HCI with surfaces and the related relaxation mechanisms, above and below the surface is presented. Extended reviews about the theoretical models are already available (e.g. [13] and references therein).

2.1. Over-the-barrier model and sub-surface relaxation

The well-established model for describing the relaxation of HCI with a metal surface is the 'classical over-the-barrier' (COM) model proposed by Burgdörfer *et al* [14–16]. In this model the neutralization of an HCI proceeds in four main steps: (a) as the ion approaches the surface, electron transfer to highly excited states of the projectile occurs resonantly 'above-the-barrier' and a 'hollow atom' (or 'hollow ion' if not fully neutralized) (HA) is formed with empty inner shells. (b) The de-excitation of the HA continues by Auger electron emission, auto-ionization and radiative decay processes still above the surface. However, the relaxation is not finished until the HA enters the surface. (c) At the impact of the HA on the surface, the electrons which are still in highly excited states are screened and 'peeled off'. (d) Finally, the neutralization of the ion continues now below the surface by direct electron transfer into inner unbound states of the ion from the bands of the solid and de-excitation by Auger electron emission and radiative emission, respectively [17, 18]. During all these processes electrons are extracted from the surface and emitted from the projectile into the vacuum or back to the surface. The majority of these electrons have energies below 20 eV. However, a few high energetic Auger electrons are also participating when empty inner shells are involved [19].

From measurements of secondary electron yields and potential energy retention it is known that the major part of the potential energy (between 70% and 90%) is deposited into the solid, at least for medium charge states ($q < 10$) and low atomic number projectiles (Ar) [20]. At higher charge states and heavier projectiles this amount might be reduced by the additional channel of x-ray emission [21]. In conclusion, two main effects are responsible for the potential energy induced excitation: the local charging of the surface by hole creation and a high electron–hole density created by inelastic collisions of electrons excited in the solid. Due to the fast relaxation of the HA or HI below the surface the energy will be deposited only in a shallow depth region, much less than the penetration depth of the ions.

2.2. Potential sputtering

Strongly connected to the surface modifications, which will be presented below, is the sputtering resulting from the electronic excitation by HCI, called *potential sputtering* (for a recent review see [8] and references therein). This sputtering process is characterized by a strong dependence of the observed sputtering yields on the charge state of the impinging ion and can already take place at ion impact energies well below the kinetic sputtering threshold. Potential sputtering yields can be orders of magnitude higher than kinetic sputtering yields at low energy which are of the order of a few atoms per ion only. Often the secondary ion yields are higher for HCI and depend on the charge state of the ions [22, 23]. For instance, for well-defined Si surfaces, i.e. hydrogen and fluorine terminated, a strong dependence ($\sim q^5$) of the H^+ and F^+ sputtering yield with charge state has been found [24, 25].

Accurate determination of the total sputter yields (including both neutral and ionized secondary particles) can be performed by means of a sensitive quartz crystal micro-balance technique [26, 27]. For conducting surfaces no charge state-dependent total sputter yield was observed (only kinetic sputtering) [28, 29]. For alkali halide and some other insulating surfaces a sizeable sputtering yield could be observed down to very low impact energies [26, 29, 30], which increased dramatically with the potential energy carried by the projectile, leading to neutral sputtering yields as high as several hundred target particles per single ion impact. In the case of an LiF surface an experimentally observed minimum potential energy (i.e. potential energy threshold) necessary for potential sputtering to occur gave a strong hint on the responsible sputtering mechanism, namely 'defect-mediated desorption' [29, 31].

3. Surface modifications induced by HCI

Studies of surface modifications induced by HCI have been conducted since high-performance sources, i.e. electron cyclotron resonance ion sources (ECRIS) and electron beam ion sources (EBIS), for extracting high charge state ion beams became available. Combined with the emergence of scanning probe techniques [32], like scanning tunneling microscopy (STM) and atomic force microscopy (AFM), in contact

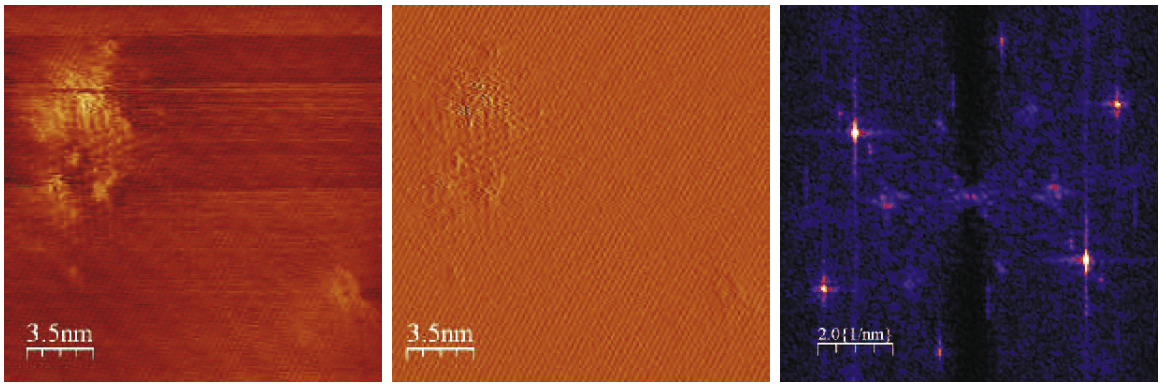

Figure 2. STM images of (1000)HOPG in constant current mode (left), constant height mode (middle) and related Fourier transform (right) cleaved in air and subsequently irradiated with Ar^{13+} at 1 keV kinetic energy.

(c-AFM) and non-contact (nc-AFM) mode, respectively, modifications induced by the impact of single HCI could be analyzed in detail. Thereby the main interest was to study the modifications induced by the potential energy of the HCI and to clarify the mechanism leading to these modifications. In the following we will review some results on different materials, mainly focusing on the systematic studies performed for CaF_2 and KBr.

3.1. Layered materials

Mica. Muscovite mica (a phyllosilicate with the sum formula $KAl_2(Si_3Al)O_{10}(OH)_2$) was the first material which has been studied after irradiation with HCI [33–36]. 'Blister'-like features have been identified on the surface of mica in c-AFM after irradiation with Kr^{35+}, Xe^{44+}, Th^{74+} and U^{70+} at a kinetic energy of 7 kV $\times$ q [33]. The lateral size of the structures is clearly increasing with the potential energy of the ions from 10 to 50 nm, thus demonstrating a potential energy induced effect [35]. The height seems to be constant at a value of 0.5–1 nm. These first experiments were performed at relatively high kinetic energy of up to 490 keV. Therefore, an unambiguous separation of kinetic and potential effects was not possible. Irradiation with Xe^{44+} at a lower kinetic energy of 44 keV resulted in formation of pit structures [34].

In general, the structures on mica seem to be not very stable and repeated scanning with the c-AFM tip over the same place changes them, i.e. flattens, erases or peels off the top layer [33, 36].

HOPG. Similar to mica, highly oriented pyrolitic graphite (HOPG) has a layered structure and the preparation of flat and clean (1000) surfaces is easy and possible in air as well. Although (1000)HOPG has a high conductivity parallel to the graphite layers the electronic excitation seems to be confined enough to produce modifications by the potential energy of HCI [37–41]. Structures were observed mainly in STM as protrusions with 0.3–1 nm height and 1–10 nm diameter. In figure 2 STM images of a defect created by a single Ar^{13+} are shown. The height of the structures is typically 0.5 nm, almost independent of the charge state, whereas the diameter increases strongly with the potential energy from 1 to 8 nm [42]. As for the kinetic energy dependence no increase in lateral size or height in the range of 1–300 keV has been observed. A $\sqrt{3} \times \sqrt{3} - R30°$ reconstruction is often observed around the defects [43]. In the early stage of investigations these defects could easily be observed with STM but were transparent for AFM because of the lower lateral resolution of the AFM tip [37]. However, recent experiments with STM and nc-AFM of the same feature have shown that the protrusions can be observed with AFM as well, at least for ions in higher charge states [39].

Molecular dynamics (MD) simulations suggest that single or complex vacancies and interstitial atom clusters are forming the observed protrusions [44]. The defects created by the irradiation with HCI could also be identified in Raman spectroscopy as an additional band originating from a disorder breathing mode, called a D peak, arising at 1355 nm^{-1} [40, 41]. From detailed analysis of the Raman spectra it was concluded that for HCI irradiation complex vacancies are the dominant defect structures [45]. As an interesting application it was demonstrated that the defects induced by HCI on HOPG can be transformed by subsequent irradiation with electrons (from the STM tip) or photons (Cd–Te laser) to sp^3 graphite, i.e. to nanoscaled diamond structures [46–48]. Recently, these modifications could be found also in simulations of the impact of highly charged Ar ions on graphite using time-dependent density functional theory combined with MD [49].

3.2. Metals and semiconductors

Because of the absence of potential sputtering yield in metallic and semiconductor surfaces it would be expected that HCI do not create any defects on these surfaces. On metals no potential energy induced structures were reported so far. However, surprisingly on Si surfaces nanostructures due to the impact of HCI have been reported in the literature (see below).

Au(111). On a clean, atomically flat Au(111) surface irradiated with Xe^{25+} and Xe^{55+} at 8 keV $\times$ q kinetic energy, islands and coexisting craters have been found with *in situ* STM [50, 51]. The study of these structures, however, revealed that they are supposedly induced by the kinetic energy and not by the potential energy of the HCI [52]. This is consistent with

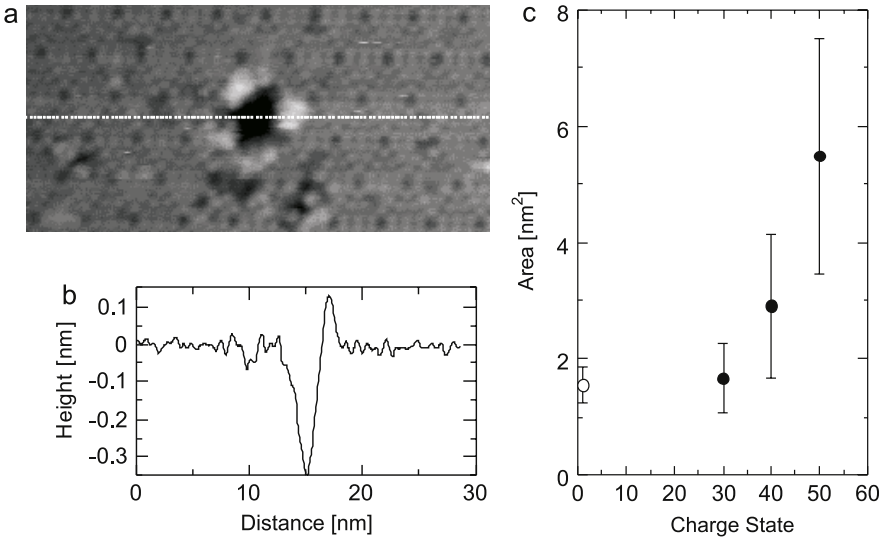

Figure 3. (a) STM image of Si(111)-(7 × 7) with an impact site of an I^{50+} ion at 150 keV kinetic energy. (b) Line profile along the crater in (a). (c) Area of the crater on Si(111) induced by I^{q+} ions as a function of the charge state q (courtesy of Tona) [53].

the assumption that a fast relaxation of the electronic excitation which, in metals, is of the order of less than 100 fs will inhibit a phase transformation.

Si(111). A different behavior was observed on Si surfaces irradiated with HCI from the Tokyo EBIT. Tona *et al* also used an *in situ* STM to observe the modifications on Si(111)-(7 × 7) induced by highly charged I^{q+} ions with charge states q of 30, 40 and 50 with atomic resolution [53–55]. At kinetic energies of 3 keV × q the I^{q+} ions produce crater-like structures with a diameter of 1.5–3 nm. In figure 3 a such a crater produced by the highest charged ion I^{50+} is shown. Around the hole in the center, which reaches a depth of 0.35 nm (as seen in figure 3(b)), brighter sites are observed in STM. From the crater size it was estimated that at least 50 Si atoms were removed by an I^{50+} ion. Figure 3(c) shows the dependence of the crater area with the charge state of the I^{q+} ions. A strong increase with the potential energy is evident.

Earlier, irradiation of clean Si(100) with highly charged Xe^{q+} ions (with q up to 44) were also reported to produce craters with a diameter of 15 nm at the highest charge state [56]. The potential sputtering yield measured on a catcher foil was 100 Si atoms for this charge state. In addition, the authors measured the photoluminescence from the irradiated surface and found additional peaks at ∼2 eV which could be assigned to excitons localized in the individual impact sites of the HCI.

3.3. Insulators

On insulators the electronic excitation induced by HCI is strongly confined. Therefore, permanent modifications are expected resulting from HCI impact on these surfaces.

Oxides. The surfaces of different oxides have been investigated by AFM and STM after the irradiation with HCI, among them Al_2O_3, SiO_2 and TiO_2. The structures on Al_2O_3 produced by 500 eV Ar^{7+} were a few nm high and up to several tens of nm in diameter [57]. However, the efficiency of the formation of these structures was estimated to be only 1/5000 and no systematic study of the size dependence on the potential energy has been done so far. Similar results were obtained on SiO_2. Another oxide which has been studied recently after irradiation with HCI is TiO_2 [58]. On the atomically flat TiO_2(110) surface two types of structures were observed after the irradiation with I^{51+} at 150 keV: hillock-like and 'caldera'-like structures. The number of structures agreed with the applied ion fluence. The crater of the caldera structures was found to be at least 1.5 nm deep, corresponding to several atomic layers. The height of the hillocks and of the rims around the crater was determined to be around 1 nm and the diameter about 10 nm at the highest charge state applied.

CaF_2. CaF_2 is an ionic crystal and a wide bandgap insulator. The best cleavage plane is the (111) which has therefore been used for experiments with HCIs. The surface, cleaved in air and then transferred to the UHV chamber, exhibits atomically flat terraces larger than 1 μm width separated by mono-atomic steps. On these fluorine terminated terraces modifications induced by HCI can easily be detected with c-AFM. Impacts of HCI on the CaF_2 surface produces hillocks with a typical height of ∼1 nm and a diameter of 20–90 nm (see figure 4(a)), depending strongly on the potential energy of the ions [59].

A remarkable observation on the formation of these hillocks on CaF_2 is a sharp, well-defined threshold in the potential energy of the HCI. Systematic studies of the hillock formation on CaF_2 with $10q$ × keV Xe^{q+} (q = 22–48) and Ar^{q+} (q = 11–18) revealed a potential energy threshold of 14 keV for hillock formation [59] which shifted to 12 keV for very slow ($150q$ × eV) HCI impact energies [60]. For potential energies smaller than the threshold no structures are found after irradiation. In figure 4(b) the hillock volume is plotted as a

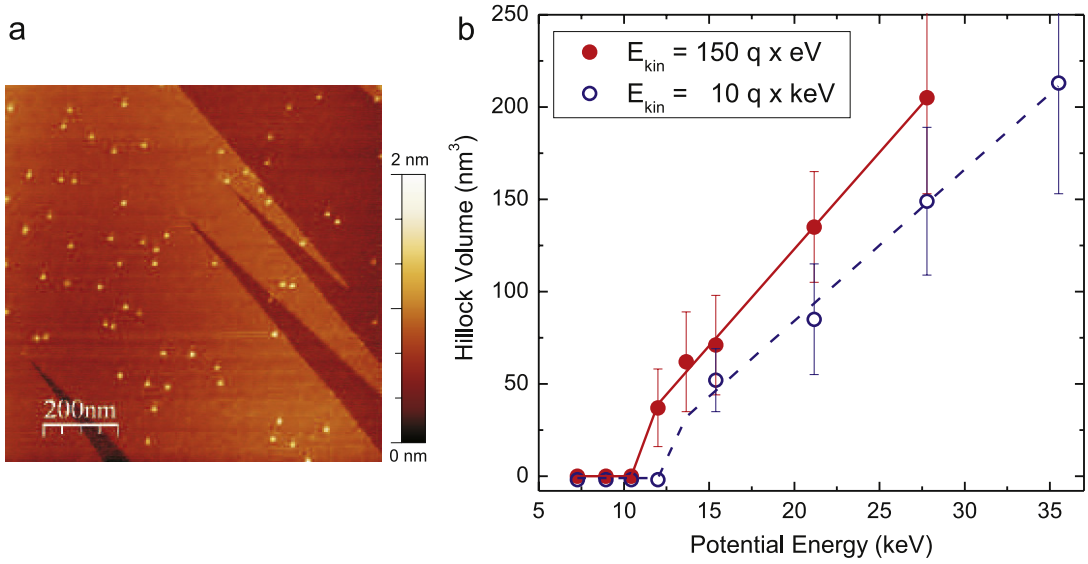

Figure 4. (a) c-AFM image of hillock structures created by the impact of highly charged Xe^{33+} ions with a kinetic energy of 66 keV on a $CaF_2(111)$ surface (scan size is 1 μm × 1 μm). (b) Mean volume of hillock-like nanostructures on a CaF_2 surface as a function of the potential energy of Xe^{q+} ions. Solid symbols correspond to measurements taken at 150 × q eV impact energies, while open symbols show the results taken for 10q × keV. Hillocks are found only above a potential energy threshold which slightly shifts with kinetic energy [60].

function of the potential energy, where the onset of hillock formation is found between charge state 27 and 28 for Xe ions. The threshold could be successfully explained by a fast solid–liquid phase transformation in a very small volume induced by the potential energy deposition. The inelastic thermal spike model (see details below) has been adapted to this case and predicted a threshold for this phase transition fairly close to the experimental finding [59]. For the highest charge states a second regime is found characterized by a steeper increase of the hillock volume with potential energy. This regime beginning at ∼50 keV could be assigned to the sublimation threshold of CaF_2 [59].

The kinetic energy shows no, or only minor, effects on the hillock volume [60]. However, recent systematic investigations at lower kinetic energies revealed that the threshold for the hillock formation is slightly shifted to lower potential energy and that the hillock volume increases slightly with decreasing kinetic energy. This observation could also be explained qualitatively by detailed simulation of the energy transfer to the lattice and the following heating and melting of the crystal. At higher kinetic energy the 'hot region' of melting protrudes deeper into the solid, thus leaving a smaller surface area affected [60].

KBr. Recently, KBr, another wide bandgap insulator, has been investigated after irradiation with slow HCI [61]. For the alkali-halide KBr the (001) surface is an easy cleavage plane and has been investigated after the impact of highly charged Xe^{q+} (q = 4–36) ions from the Dresden EBIT [62]. With c-AFM pit structures have been identified on the irradiated surfaces with a density corresponding to the applied ion fluence. The pits formed by every incident ion are only 1 ML deep (0.35 nm) with a diameter of 10–20 nm increasing with the potential energy. They are formed by the simultaneous desorption of up to 2700 atoms (at the highest charge state of Xe^{36+} used in the experiments) from one impact site. Similar to the case of hillock formation on CaF_2 a threshold for the formation of these pits has been found above Xe^{10+} corresponding to a potential energy of ∼1.5 keV [61]. In figure 5(a) a c-AFM image of pits formed on a cleaved KBr surface by Xe^{30+} ions is shown. Figure 5(b) displays the pit volume as a function of the potential energy of the Xe ions. The kinetic energy of the Xe ions was kept constant at 40 keV for these measurements.

Studying the emergence of the pit structures on KBr in more detail as a function of the potential and kinetic energy of the HCI a surprising behavior was found: a second threshold in the kinetic energy of the ions exists which decreases with the charge states of the ions. This clearly indicates a synergistic excitation of the surface by the kinetic and potential energy, respectively. In figure 6 a 'phase diagram' for the formation of pit structures on KBr is shown. From the phase diagram it can be concluded that the formation of the pit structures on KBr is not effected by the potential energy alone. It has to be assumed, therefore, that kinetically induced defects created in the collision cascade amplify the trapping of the electron–hole pairs created by the potential energy. This kind of synergism has already been observed in the potential sputtering yield of MgO and Al_2O_3 [63]. In these cases the effect was termed 'kinetically assisted potential sputtering' and was attributed to this seeding effect of the electron–hole trapping. In order to clarify the role of the kinetic induced effects in the formation mechanism of the pit structures on KBr more systematic investigations are needed.

4. Models of surface modification by HCI

Different models have been proposed to explain the surface modifications observed after the irradiation with HCI. These

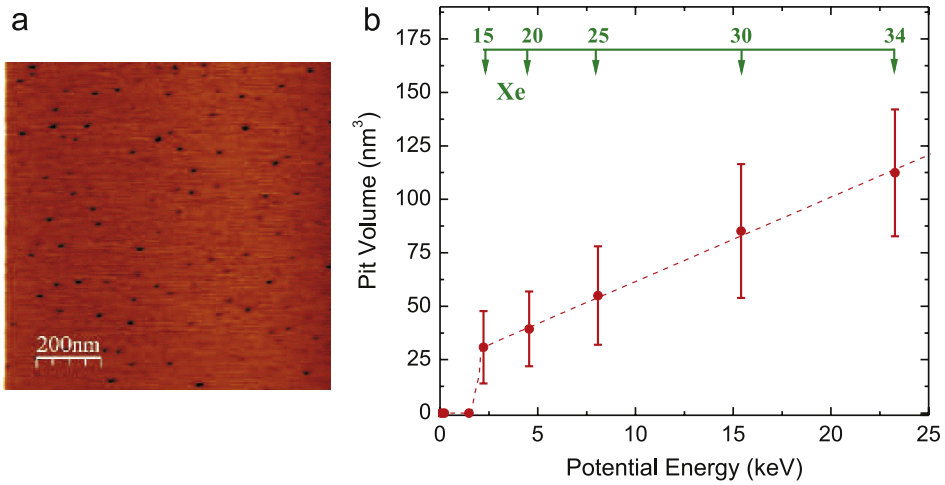

Figure 5. (a) c-AFM image of pit structures created on a KBr(001) surface by the impact of highly charged Xe^{30+} ions with a kinetic energy of 40 keV and fluence of 7×10^9 cm^{-2} (scan size is 1 μm $\times$ 1 μm). (b) Volume of pit structures on KBr surfaces induced by highly charged Xe ions as a function of their potential energy [61].

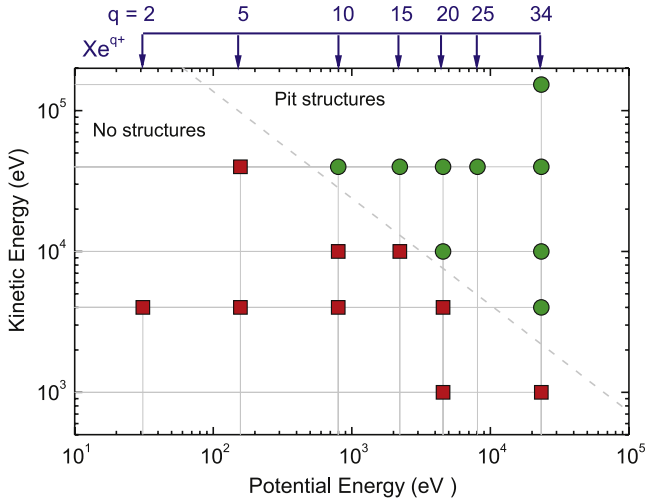

Figure 6. 'Phase diagram' of the emergence of pit structures on KBr surfaces induced by highly charged Xe ions as a function of potential and kinetic energy.

models have already been used for the interpretation of potential sputter yield measurements. In the following they are introduced briefly and applied to the respective system.

4.1. Coulomb explosion

The interaction of HCI with surfaces includes charge exchange processes which extract a large amount of electrons from the solid surface. For instance, a Xe^{40+} needs 40 electrons to be neutralized and will eject approx. 100 additional secondary electrons [64]. Hence, a small volume around the impact site will be depleted by ~140 electrons. As a consequence, the Coulomb explosion model, first proposed for HCI-induced effects by Parilis *et al* [65–67], has been considered frequently for the explanation of the observed modification by HCI. The blister structures formed on mica, for instance, were attributed to the electrostatic Coulomb repulsion connected to the charge accumulation [67]. Similarly, the crater structures formed on Si have been assigned to the fast evaporation of Si atoms resulting from the shockwave in a Coulomb explosion. The detailed molecular dynamic simulations demonstrate that more than 250 Si ions are produced under the surface by a single HCI impact [66]. The average energy of the emitted ions was estimated to 100 eV.

However, careful analysis of the experimental results on potential sputtering yield and theoretical estimates lead to the conclusion that the Coulomb explosion is not the dominant mechanism, but rather defect-mediated desorption is more probable in most of the cases [31, 8]. Some special cases exist where the experiments are in good agreement with theoretical calculation based on Coulomb explosion, i.e. sputtering of H-terminated or hydrocarbon-terminated Si surfaces.

4.2. Defect-induced desorption

Defect-induced desorption had been recognized already in the 1970s as the primary mechanism for the electron and photon stimulated desorption from alkali halides [68]. In the case of HCI interacting with a surface holes and electron–hole pairs are created in the valence band following the neutralization and relaxation of the ion. If the coupling to the lattice is strong enough, as in the case of alkali halides, the holes and e–h pairs are trapped, forming so-called *self-trapped holes* (STH) or *self-trapped excitons* (STE). The STE decay further into color centers forming H centers, i.e. interstitial molecular halide ions, and F centers, i.e. electrons at anion sites. The H centers are mobile, can reach the surface and the desorption of a halide atom is initiated [69]. F centers are not as mobile as the H centers but can also reach the surface. However, an energy deficiency is inhibiting the thermal desorption of an neutralized alkali ion from the crystal [70]. Only if the F center is excited or the relaxation takes place at a low coordinated site, like a step edge, then the alkali atoms can be desorbed. However, when several defects are created in a small volume complex defect centers (X centers) are formed and the desorption of

halide and alkali atoms can take place. This is very probable for the HCI interaction with an alkali-halide surface as has been pointed out earlier. The high electronic excitation would then initiate the simultaneous desorption of numerous atoms from the surface, leading to the formation of a pit structure.

The defect-induced desorption model is probable for all crystal where a strong electron–phonon coupling is present, e.g. in the above treated alkali halides, oxides, oxidized surfaces or some semiconductors. This model has also been identified as the origin for the potential sputtering yield observed on LiF, SiO_2 and Al_2O_3.

4.3. Thermal spike model

In the case of the formation of hillocks on the irradiated CaF_2 surfaces the 'inelastic thermal spike model' by Toulemonde *et al* has been successfully applied [60]. This model had originally been developed for the creation of hillocks by swift heavy ions which have kinetic energies exceeding 100 keV amu^{-1} [71]. For these ions the electronic stopping dominates the energy dissipation of the ions and the material is highly excited along the 'ion tracks'. In these tracks the material is rapidly heated by energetic electrons transferring their energy to the lattice atoms. Accordingly, the lattice melts, if the local lattice temperature rises above the melting point. Discontinuous or continuous amorphous tracks are observed after the irradiation with SHI in the bulk of the solid or at the surface [72] when the electronic energy loss exceeds the value of ∼5 keV nm^{-1} [73]. The hillocks are then created due to relaxation of the internal stress produced by the SHI.

For HCI the thermal spike model has to be modified slightly [60, 74]. Here, the fundamentally different excitation by the HCI has to be taken into account. This can be done by using the COM model for the neutralization of HCI. This model is able to explain the observed threshold for the hillock formation. As a nice result it also predicts the threshold between Ar^{17+} and Ar^{18+} which was somewhat puzzling because only an additional high energy KLL electron is involved which might also escape during the relaxation [74].

5. Summery and outlook

We have presented an overview of this rapidly evolving field of surface modifications induced by the potential energy of HCI. As a general rule it can already be stated that in solids where the electronic excitation induced by HCI is confined and cannot relax rapidly the impact of HCI can create permanent modifications on the surface. These structures can be observed and analyzed in detail by scanning probe microscopy. The volume of the structures show a pronounced dependence on the potential energy. In many materials a threshold in the potential energy for the formation of structures has been clearly identified or suspected. This suggests that a minimum energy density is needed to induce permanent phase transformations.

The models to explain the formation of the hillock and pit structures, respectively, are not fully developed yet, but give some fairly good qualitative agreement with the experimental observations. Still, however, no unified picture of the excitation and modification induced by HCI is available. Therefore, more systematic investigations are needed on different materials and with different projectiles, i.e. atomic number, charge state and kinetic energy. In order to rule out any kinetic-induced effects slow HCI with kinetic energies <10 keV should be used. This can be achieved by deceleration of the ion beams from the ECR or EBIT sources.

As has already been recognized in the last few years clean atomically flat surfaces are needed in order to clearly identify and analyze the surface modifications. Therefore, preparation techniques and ultra-high vacuum conditions, as usual in the surface science community, have to be applied. In addition, as exposure to air after the irradiation could eventually change or even induce modifications, it is highly recommended to transfer the samples without breaking vacuum. This can be accomplished by *in situ* STM/AFM or by transfer via a vacuum suitcase.

Acknowledgments

This work has been supported by the European ITS LEIF network (contract no. RII3#026015), by the European network RITA (contract no. 025646) and by the Austrian Science Foundation FWF. The authors acknowledge discussions with Joachim Burgdörfer, Christoph Lemell, Christina Trautmann, Marcel Toulemonde and Wolfhard Möller.

References

[1] Chason E *et al* 1997 Ion beams in silicon processing and characterization *J. Appl. Phys.* **81** 6513–61
[2] Chan W L and Chason E 2007 Making waves: kinetic processes controlling surface evolution during low energy ion sputtering *J. Appl. Phys.* **101** 121301
[3] Gnaser H 1999 *Low-Energy Ion Irradiation of Solid Surfaces* (*Springer Tracts in Modern Physics* vol 146) (Berlin: Springer)
[4] Arnau A *et al* 1997 Interaction of slow multicharged ions with solid surfaces *Surf. Sci. Rep.* **27** 117–239
[5] Delaunay M, Fehringer M, Geller R, Hitz D, Varga P and Winter H 1987 Electron-emission from a metal-surface bombarded by slow highly charged ions *Phys. Rev.* B **35** 4232–5
[6] Aumayr F, Kurz H, Schneider D, Briere M A, Mcdonald J W, Cunningham C E and Winter H P 1993 Emission of electrons from a clean gold surface-induced by slow, very highly-charged ions at the image charge acceleration limit *Phys. Rev. Lett.* **71** 1943–6
[7] Aumayr F and Winter H 2007 Potential electron emission from metal and insulator surfaces *Slow Heavy-Particle Induced Electron Emission from Solid Surfaces* (*Springer Tracts in Modern Physics* vol 225) ed H P Winter and J Burgdörfer (Berlin: Springer) pp 79–112
[8] Aumayr F and Winter H 2004 Potential sputtering *Phil. Trans. R. Soc.* A **362** 77–102
[9] Aumayr F, El-Said A S and Meissl W 2008 Nano-sized surface modifications induced by the impact of slow highly charged ions-a first review *Nucl. Instrum. Methods* B **266** 2729–35
[10] Schenkel T, Hamza A V, Barnes A V, Schneider D H, Walsh D S and Doyle B L 1998 Analysis of B–SiO_2 films by highly charged ion based time-of-flight secondary ion mass spectrometry, standard secondary ion mass spectrometry and elastic recoil detection *J. Vac. Sci. Technol.* A **16** 1384–7

[11] Aumayr F and Winter H P 2003 Slow highly charged ions-a new tool for surface nanostructuring? *e-J. Surf. Sci. Nanotechnol.* **1** 171–4

[12] Schenkel T, Persaud A, Park S J, Meijer J, Kingsley J R, McDonald J W, Holder J P, Bokor J and Schneider D H 2002 Single ion implantation for solid state quantum computer development *J. Vac. Sci. Technol.* B **20** 2819–23

[13] Winter H P and Burgdörfer J 2007 *Slow Heavy-Particle Induced Electron Emission from Solid Surfaces* (*Springer Tracts in Modern Physics* vol 225) (Berlin: Springer)

[14] Burgdörfer J, Lerner P and Meyer F W 1991 Above-surface neutralization of highly charged ions-the classical over-the-barrier model *Phys. Rev.* A **44** 5674–85

[15] Burgdörfer J and Meyer F 1993 Image acceleration of multiply charged ions by metallic surfaces *Phys. Rev.* A **47** R20–2

[16] Lemell C, Winter H P, Aumayr F, Burgdörfer J and Meyer F 1996 Image acceleration of highly charged ions by metal surfaces *Phys. Rev.* A **53** 880–5

[17] Stolterfoht N, Arnau A, Grether M, Kohrbruck R, Spieler A, Page R, Saal A, Thomaschewski J and Bleckneuhaus J 1995 Multiple-cascade model for the filling of hollow Ne atoms moving below an Al surface *Phys. Rev.* A **52** 445–56

[18] Pesic Z D, Vikor G, Atanassova S, Anton J, Leontein S, Bjorkhage M, Paal A, Hanafy H and Schuch R 2007 Relaxation of slow highly charged ions hitting thin metallic foils *Phys. Rev.* A **75** 11

[19] Niemann D, Grether M, Spieler A, Stolterfoht N, Lemell C, Aumayr F and Winter H P 1997 Emission of low-energy electrons from slow N^{6+} ions interacting with a Au surface *Phys. Rev.* A **56** 4774–80

[20] Kost D, Facsko S, Moller W, Hellhammer R and Stolterfoht N 2007 Channels of potential energy dissipation during multiply charged argon-ion bombardment of copper *Phys. Rev. Lett.* **98** 225503

[21] Watanabe H, Takahashi S, Tona M, Yoshiyasu N, Nakamura N, Sakurai M, Yamada C and Ohtani S 2006 Dissipation of potential energy through x-ray emission in slow highly charged ion-surface collisions *Phys. Rev.* A **74** 042901

[22] Schenkel T, Barnes A V, Hamza A V, Schneider D H, Banks J C and Doyle B L 1998 Synergy of electronic excitations and elastic collision spikes in sputtering of heavy metal oxides *Phys. Rev. Lett.* **80** 4325–8

[23] Schenkel T, Schneider M, Hattass M, Newman M W, Barnes A V, Hamza A V, Schneider D H, Cicero R L and Chidsey C E D 1998 Electronic desorption of alkyl monolayers from silicon by very highly charged ions *J. Vac. Sci. Technol.* B **16** 3298–300

[24] Kuroki K, Okabayashi N, Torii H, Komaki K and Yamazaki Y 2002 Potential sputtering of proton from hydrogen-terminated Si(100) surfaces induced with slow highly charged ions *Appl. Phys. Lett.* **81** 3561–3

[25] Okabayashi N, Komaki K and Yamazaki Y 2005 Energy- and angular-distributions of F+ ions emitted from a F-terminated Si(100) surface with slow highly charged ions *Nucl. Instrum. Methods* B **235** 438–42

[26] Neidhart T, Pichler F, Aumayr F, Winter H P, Schmid M and Varga P 1995 Potential sputtering of lithium-fluoride by slow multicharged ions *Phys. Rev. Lett.* **74** 5280–3

[27] Hayderer G, Schmid M, Varga P, Winter H P and Aumayr F 1999 A highly sensitive quartz-crystal microbalance for sputtering investigations in slow ion-surface collisions *Rev. Sci. Instrum.* **70** 3696–700

[28] Varga P, Neidhart T, Sporn M, Libiseller G, Schmid M, Aumayr F and Winter H P 1997 Sputter yields of insulators bombarded with hyperthermal multiply charged ions *Phys. Scr.* T **73** 307–10

[29] Hayderer G, Schmid M, Varga P, Winter H P, Aumayr F, Wirtz L, Lemell C, Burgdörfer J, Hagg L and Reinhold C O 1999 Threshold for potential sputtering of LiF *Phys. Rev. Lett.* **83** 3948–51

[30] Sporn M, Libiseller G, Neidhart T, Schmid M, Aumayr F, Winter H P, Varga P, Grether M, Niemann D and Stolterfoht N 1997 Potential sputtering of clean SiO_2 by slow highly charged ions *Phys. Rev. Lett.* **79** 945–8

[31] Aumayr F, Burgdörfer J, Varga P and Winter H P 1999 Sputtering of insulator surfaces by slow highly charged ions: 'coulomb explosion' or 'defect mediated desorption'? *Comments At. Mol. Phys.* **34** 201–19

[32] Binning G, Rohrer H, Gerber C and Weibel E 1982 Surface studies by scanning tunneling microscopy *Phys. Rev. Lett.* **49** 57–61

[33] Schneider D H, Briere M A, Mcdonald J and Biersack J 1993 Ion surface interaction studies with 1–3 keV amu^{-1} ions up to Th^{80+} *Radiat. Eff. Defects Solids* **127** 113–36

[34] Parks D C, Bastasz R, Schmieder R W and Stockli M 1995 Nanometer-size surface-features produced by single, low-energy, highly-charged ions *J. Vac. Sci. Technol.* B **13** 941–8

[35] Ruehlicke C, Briere M A and Schneider D 1995 Afm studies of a new-type of radiation defect on mica surfaces caused by highly-charged ion impact *Nucl. Instrum. Methods* B **99** 528–31

[36] Parks D C, Stockli M P, Bell E W, Ratliff L P, Schmieder R W, Serpa F G and Gillaspy J D 1998 Non-kinetic damage on insulating materials by highly charged ion bombardment *Nucl. Instrum. Methods* B **134** 46–52

[37] Mochiji K, Yamamoto S, Shimizu H, Ohtani S, Seguchi T and Kobayashi N 1997 Scanning tunneling microscopy and atomic force microscopy study of graphite defects produced by bombarding with highly charged ions *J. Appl. Phys.* **82** 6037–40

[38] Hayderer G, Cernusca S, Schmid M, Varga P, Winter H P and Aumayr F 2001 Stm studies of Hcl-induced surface damage on highly oriented pyrolytic graphite *Phys. Scr.* T **92** 156–7

[39] Terada M, Nakamura N, Nakai Y, Kanai Y, Ohtani S, Komaki K and Yamazaki Y 2005 Observation of an HCI-induced nano-dot on an HOPG surface with STM and AFM *Nucl. Instrum. Methods* B **235** 452–5

[40] Tona M, Baba Y, Takahashi S, Nagata K, Nakamura N, Yoshiyasu N, Yamada C and Ohtani S 2005 *In* and *ex situ* optical spectroscopy of HCI-bombarded solid surfaces *Nucl. Instrum. Methods* B **235** 443–7

[41] Baba Y, Nagata K, Takahashi S, Nakamura N, Yoshiyasu N, Sakurai M, Yamada C, Ohtani S and Tona M 2005 Surface modification on highly oriented pyrolytic graphite by slow highly charged ions *Surf. Sci.* **599** 248–54

[42] Nakamura N, Terada M, Nakai Y, Kanai Y, Ohtani S, Komaki K and Yamazaki Y 2005 SPM observation of nano-dots induced by slow highly charged ions *Nucl. Instrum. Methods* B **232** 261–5

[43] Gebeshuber I C, Cernusca S, Aumayr F and Winter H P 2003 Nanoscopic surface modification by slow ion bombardment *Int. J. Mass Spectrom.* **229** 27–34

[44] Nordlund K, Keinonen J and Mattila T 1996 Formation of ion irradiation induced small-scale defects on graphite surfaces *Phys. Rev. Lett.* **77** 699

[45] Hida A, Meguro T, Maeda K and Aoyagi Y 2003 Analysis of surface modifications on graphite induced by slow highly charged ion impact *Nucl. Instrum. Methods* B **205** 736–40

[46] Meguro T, Hida A, Suzuki M, Koguchi Y, Takai H, Yamamoto Y, Maeda K and Aoyagi Y 2001 Creation of nanodiamonds by single impacts of highly charged ions upon graphite *Appl. Phys. Lett.* **79** 3866–8

[47] Meguro T, Hida A, Koguchi Y, Miyamoto S, Yamamoto Y, Takai H, Maeda K and Aoyagi Y 2003 Nanoscale transformation of sp(2) to sp(3) of graphite by slow highly charged ion irradiation *Nucl. Instrum. Methods* B **209** 170–4

[48] Sideras-Haddad E, Schenkel T, Shrivastava S, Makgato T, Batra A, Mwakikunga B, Erasmus R and Persaud A 2008 *ICACS 2008 Nucl. Instrum. Methods* B submitted

[49] Miyamoto Y 2007 Ultrafast reconstruction of graphite by irradiating with highly charged ions *Appl. Phys. Lett.* **91** 3
[50] Pomeroy J M, Grube H, Perrella A C and Gillaspy J D 2007 Stm and transport measurements of highly charged ion modified materials *Nucl. Instrum. Methods* B **258** 189–93
[51] Pomeroy J M, Grube H, Perrella A C, Sosolik C E and Gillaspy J D 2007 Transport and Stm measurements of Hci modified materials *Nucl. Instrum. Methods* B **256** 319–23
[52] Pomeroy J M, Perrella A C, Grube H and Gillaspy J D 2007 Gold nanostructures created by highly charged ions *Phys. Rev.* B **75** 241409
[53] Tona M, Watanabe H, Takahashi S, Nakamura N, Yoshiyasu N, Sakurai M, Terui T, Mashiko S, Yamada C and Ohtani S 2007 Nano-crater formation on a Si(111)-(7 × 7) surface by slow highly charged ion-impact *Surf. Sci.* **601** 723–7
[54] Tona M, Watanabe H, Takahashi S, Nakamura N, Yoshiyasu N, Sakurai M, Terui T, Mashiko S, Yamada C and Ohtani S 2007 Nanofabrication on a Si surface by slow highly charged ion impact *Nucl. Instrum. Methods* B **256** 543–6
[55] Tona M, Watanabe H, Takahashi S, Nakamura N, Yoshiyasu N, Sakurai M, Yamada C and Ohtani S 2007 Potential sputtering from a Si surface by very highly charged ion impact *Nucl. Instrum. Methods* B **258** 163–6
[56] Hamza A V, Newman M W, Thielen P A, Lee H W H, Schenkel T, McDonald J W and Schneider D H 2001 Light-emitting nanostructures formed by intense, ultrafast electronic excitation in silicon (100) *Appl. Phys. Lett.* **79** 2973–5
[57] Gebeshuber I C, Cernusca S, Aumayr F and Winter H P 2003 Afm search for slow MCI-produced nanodefects on atomically clean monocrystalline insulator surfaces *Nucl. Instrum. Methods* B **205** 751–7
[58] Tona M, Fujita Y, Yamada C and Ohtani S 2008 Electronic interaction of individual slow highly charged ions with TiO_2(110) *Phys. Rev.* B **77** 155427
[59] El-Said A S, Meissl W, Simon M C, Lopez-Urrutia J R C, Gebeshuber I C, Lang M, Winter H, Ullrich J and Aumayr F 2007 Surface nanostructures induced by slow highly charged ions on CaF_2 single crystals *Nucl. Instrum. Methods* B **256** 346–9
[60] El-Said A S *et al* 2008 Creation of nanohillocks on CaF_2 surfaces by single slow highly charged ions *Phys. Rev. Lett.* **100** 237601
[61] Heller R, Facsko S, Wilhelm R A and Möller W 2008 Defect mediated desorption of the KBr(001) surface induced by single highly charged ion impact *Phys. Rev. Lett.* **101** 096102
[62] Zschornack G, Kreller M, Ovsyannikov V P, Grossman F, Kentsch U, Schmidt M, Ullmann F and Heller R 2008 Compact electron beam ion sources/traps: review and prospects *Rev. Sci. Instrum.* **79** 02A703
[63] Hayderer G *et al* 2001 Kinetically assisted potential sputtering of insulators by highly charged ions *Phys. Rev. Lett.* **86** 3530–3
[64] Meissl W, Winklehner D, Aumayr F, Simon M C, Ginzel R, Lopez-Urrutia j R C, Ullrich J, Solleder B, Lemell C and Burgdörfer J 2008 Electron emission from insulators irradiated by slow highly charged ions *e-J. Surf. Sci. Nanotechnol.* **6** 54–9
[65] Parilis E 1996 Radiation effects under multiply charged ion impacts *Nucl. Instrum. Methods* B **116** 478–81
[66] Cheng H P and Gillaspy J D 1997 Nanoscale modification of silicon surfaces via coulomb explosion *Phys. Rev.* B **55** 2628–36
[67] Parilis E S 2001 Coulomb explosion sputtering, crater and blister formation by HCI *Phys. Scr.* T **92** 197–201
[68] Szymonski M, Kolodziej J, Postawa Z, Czuba P and Piatkowski P 1995 Electron-stimulated desorption from ionic-crystal surfaces *Prog. Surf. Sci.* **48** 83–96
[69] Szymonski M 1990 Current views on electronic and cascade sputtering of alkali-halides *Nucl. Instrum. Methods* B **46** 427–34
[70] Puchin V, Shluger A, Nakai Y and Itoh N 1994 Theoretical-study of Na-atom emission from NaCl(100) surfaces *Phys. Rev.* B **49** 11364–73
[71] Toulemonde M, Dufour C and Paumier E 1992 Transient thermal-process after a high-energy heavy-ion irradiation of amorphous metals and semiconductors *Phys. Rev.* B **46** 14362–9
[72] Akcoltekin E, Peters T, Meyer R, Duvenbeck A, Klusmann M, Monnet I, Lebius H and Schleberger M 2007 Creation of multiple nanodots by single ions *Nat. Nanotechnol.* **2** 290–294
[73] Trautmann C, Toulemonde M, Costantini J M, Grob J J and Schwartz K 2000 Swelling effects in lithium fluoride induced by swift heavy ions *Phys. Rev.* B **62** 13–6
[74] Lemell C, El-Said A S, Meissl W, Gebeshuber I C, Trautmann C, Toulemonde M, Burgdörfer J and Aumayr F 2007 On the nano-hillock formation induced by slow highly charged ions on insulator surfaces *Solid-State Electron.* **51** 1398–404